Advances in Geo-Energy Research

Vol. 6, No. 4, p. 286-295, 2022

Original article

Effect of dynamic threshold pressure gradient on production performance in water-bearing tight gas reservoir

Weiyao Zhu[1], Yuwei Liu[1], Yunqing Shi[2,3], Guodong Zou[1], Qitao Zhang[4], Debin Kong[1]*

[1]*School of Civil and Resources Engineering, University of Science and Technology Beijing, Beijing 100083, P. R. China*

[2]*Research Institute of Exploration and Production, Sinopec, Beijing 100083, P. R. China*

[3]*Key Laboratory for Marine Oil and Gas Exploitation, Sinopec, Beijing 100083, P. R. China*

[4]*John and Willie Leone Family Department of Energy and Mineral Engineering, The Pennsylvania State University, State College, 16801, USA*

Keywords:
Dynamic threshold pressure gradient
water-bearing
tight gas reservoir
production model

Cited as:
Zhu, W., Liu, Y., Shi, Y., Zou, G., Zhang, Q., Kong, D. Effect of dynamic threshold pressure gradient on production performance in water-bearing tight gas reservoir. Advances in Geo-Energy Research, 2022, 6(4): 286-295.
https://doi.org/10.46690/ager.2022.04.03

Abstract:
Water content and distribution have important impacts on gas production in water-bearing tight gas reservoirs. However, due to the structural and chemical heterogeneity of tight reservoirs, the water phase exists in various states, which has complicated the analyses of the effects of water characteristics on tight gas production performance. In this work, the water phase is distinguished from immobile to mobile states and the term of constrained water saturation is proposed. It is established that water can flow when the driving pressure difference is larger than the critical driving pressure difference. A new theoretical model of threshold pressure gradient is derived to incorporate the influences of constrained water saturation and permeability. On this basis, a new prediction model considering the varied threshold pressure gradient is obtained, and the result indicates that when threshold pressure gradient is constant, the real gas production capacity of the reservoir will be weakened. Meanwhile, a dynamic supply boundary model is presented, which indicates that the permeability has a strong influence on the dynamic supply boundary, whereas the impact of initial water saturation is negligible. These findings provide insights into the understanding of the effects of water state and saturation on the threshold pressure gradient and gas production rate in tight gas reservoirs. Furthermore, this study provides useful guidance on the prediction of field-scale gas production.

1. Introduction

Nowadays, tight gas is one of the most important unconventional energy resources (McGlade et al., 2013; Szabó et al., 2022). Meanwhile, tight sandstone reservoirs feature strong heterogeneity (Afagwu et al., 2021; Gao et al., 2021; Shilov et al., 2022), porosity that is usually less than 10%, and permeability is less than 1 mD (Shar et al., 2016; Akilu et al., 2021; Verdugo and Doster, 2022). Due to the influence of low porosity, low permeability and strong inhomogeneity, gas and water in these reservoirs are in a highly complex state of distribution (Muskat and Meres, 1936; Zou et al., 2012). Therefore, defining the characteristics of formation water distribution and flow state will enhance the study of natural gas production rules. Based on the microscopic pore structure and strong hydrophilicity of tight sandstone, formation water is divided into two types: movable water and irreducible water (Meng et al., 2016; El Sharawy and Gaafar, 2019; Mejia et al., 2021). This classification approach only considers the flow state of water, while the influence of pore throat size and driving pressure on formation water is also important.

According to previous theoretical and laboratory studies, fluid flow in tight gas reservoirs is no longer consistent with Darcy's law but conforms to the non-Darcy flow (Pertsin and Grunze, 2004), with the threshold pressure gradient (TPG) being one of the reasons for this consideration. The TPG has been extensively studied as an important feature of non-

Yandy Scientific Press

*Corresponding author.
E-mail address: weiyaook@sina.com (W. Zhu); b20170001@xs.ustb.edu.cn (Y. Liu); syq.syky@sinopec.com (Y. Shi); zouguodong@111.com (G. Zou); qpz5080@psu.edu (Q. Zhang); kongdb@ustb.edu.cn (D. Kong).

Received April 14, 2022; revised May 8, 2022; accepted May 13, 2022; available online May 15, 2022.

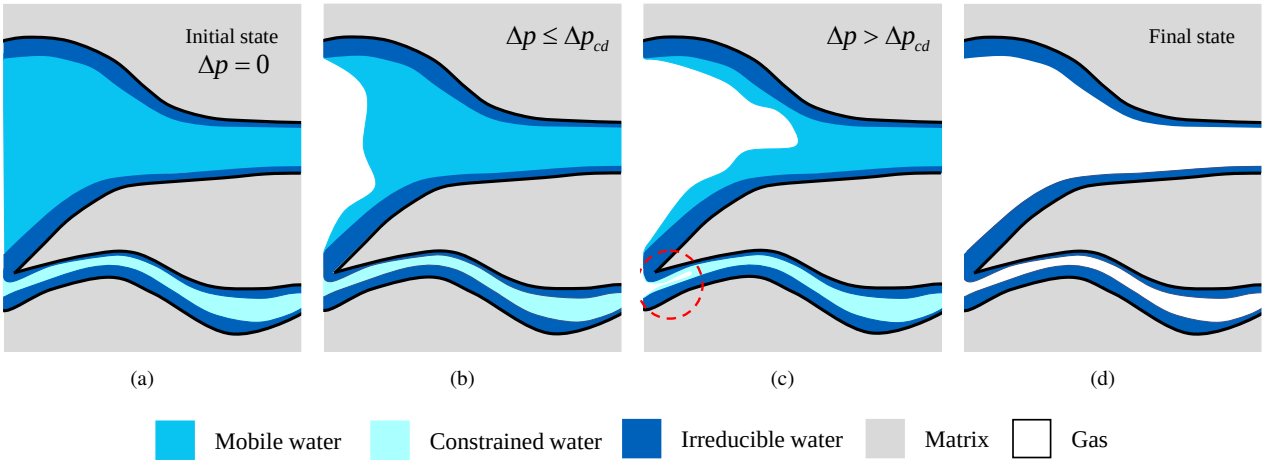

Fig. 1. States of water phase existing at various stages in tight gas reservoirs. (a) Initial stage without driving pressure difference; (b) Intermediate stage when the driving pressure is smaller than the critical driving pressure difference; (c) Immediate stage when the driving pressure is larger than the critical driving pressure difference; and (d) Final stage when all of the movable water and the constrained water have been displaced.

Darcy flow in tight gas reservoirs (Cai, 2014; Li et al., 2017; Liu et al., 2020; Ning et al., 2020). In 1963, Miller and Low (1963) performed numerous experiments on the seepage of water in low-permeability porous media, and proposed that the interaction between adsorption molecules and solid molecules leads to the existence of TPG. Subsequently, Parda and Civan (1999) modified Darcy's law using the TPG. The study by Zhu et al. (2011) showed that TPG increases with the decrease of permeability or increase of water saturation. Zeng et al. (2010) analyzed the influence of permeability and fluid components on TPG using the steady pressure-velocity method, and found that the power function is preferred for the TPG. Yang et al. (2015) carried out an experiment while combining the gas bubble method and the differential pressure flow method to investigate the TPG and non-linear seepage characteristics of a tight gas reservoir, and obtained the related function, which considered the influence of water saturation. Based on the study of factors affecting TPG, control equations considering TPG were established in conjunction with the specific conditions of the reservoir (Han et al., 2018), and these equations have been widely used in well test analysis (Guo et al., 2012) and production rate prediction (Imani et al., 2022). Thus, for a more accurate evaluation of the gas production capacity, it is necessary to consider the effect of water saturation and permeability on TPG in the prediction model of gas production performance.

Currently, there are three main methods for production rate calculation: the analytical method (Zhu et al., 2021) and numerical simulation (Zhao et al., 2020; Mahdi et al., 2021; Chai et al., 2022). The analytical solution is characterized by its computational simplicity, is suitable for solving steady-state or proposed steady-state flow problems, and is more convenient for use in the field (Kong et al., 2020). However, the analytical model has many assumptions and cannot consider certain actual situations. The numerical simulation method with commercial software can accurately describe the reservoir and fluid properties and is suitable for simulating complex flow characteristics. However, this method is computationally intensive, and the main problem to be solved is to select a suitable solution method and shorten the solution time. In this work, the production prediction model and dynamic boundary model of the water-bearing tight gas reservoir are solved based on the analytical method.

TPG is generally considered as a constant term in the calculation process, and the magnitude of its value is artificially set and is not necessarily accurate (Li et al., 2017). Therefore, based on experimental data, the present study redefined the different states of the water phase and derived a new TPG model considering the water saturation and permeability. Subsequently, the effect of TPG on gas production rate was evaluated. The findings improve the fundamental understanding of fluid flow in unconventional reservoirs and promotes the more accurate prediction of tight gas production at the reservoir scale.

2. Predictive model for TPG in tight sandstone

2.1 Definition of water in different states

According to previous studies, the state of the water phase in a reservoir is divided into movable water and irreducible water (Taktak et al., 2011; Wang and Sheng, 2017). Herein, based on the location of the existing water phase and the flow conditions, the water phase is divided into movable water, irreducible water and constrained water (Fig. 1). Water that can flow within the pore space under any driving pressure difference is defined as movable water (Hossain et al., 2011). The resulting saturation is movable water saturation (S_{wm}). Irreducible water is the water that is immovable under any conditions, and the corresponding saturation is irreducible water saturation (S_{wir}) (Durucan et al., 2014). The value of S_{wir} is constant. Constrained water constitutes the water that can only flow when the driving pressure difference is larger

than a critical value. The critical value is called critical driving pressure difference (Δp_{cd}). The ratio of constrained water volume to total water volume is defined as constrained water saturation (S_{wc}).

2.2 Analysis of constrained water

The amplitude frequency distribution curve and cumulative amplitude frequency distribution curve can be obtained by nuclear magnetic resonance (NMR) (Castro and Lupinacci, 2022). The porosity distribution curve can be acquired according to the amplitude frequency distribution curve; at the same time, the core pores can be divided into large and small pores according to the trough of the curve (Xin et al., 2022). The cumulative porosity distribution curve can be obtained from the cumulative amplitude frequency distribution curve; thus, the cumulative water saturation curve can be derived. Combining the porosity distribution curve and cumulative porosity distribution curve, the movable water saturation curve for large pores and the constrained water saturation curve for small pores can be drawn (Li et al., 2021).

Zhang et al. (2020) performed gas drive experiments on the cores after being fully saturated with water using different driving pressures for 2 hours, and then measured the core weight and performed NMR tests. According to the T2 spectrum curve, the B1 core had a T2 cutoff value of 29.67 ms and the B2 core had a T2 cutoff value of 3.85 ms, and the residual water saturation ranges from 73.64% to 55.03% for B1 and 77.13% to 69.73% for B2 when the replacement pressure is increased from 0.2 to 8 MPa. Irreducible water saturation is the water saturation at a repulsion pressure difference of 8 MPa and T2 correlation time of 10,000 ms, which gave an irreducible water saturation value of 52.51% for core B1 and 68.42% for core B2. The residual water saturation minus the irreducible water saturation will yield the constrained water saturation at different driving pressures, the results are shown in Fig. 2.

It can be seen from Fig. 2 that permeability is inversely proportional to constrained water saturation. Based on the above curve characteristics, the solution equation of constrained water saturation can be obtained by the nonlinear regression method, thus the constrained water saturation equation is established empirically by Eq. (1).

$$S_{wc} = A(k_0) \cdot \ln(\Delta p) + B(k_0) \tag{1}$$

where k_0 denotes the permeability, mD; $A(k_0)$ and $B(k_0)$ are the coefficients related to permeability; Δp denotes the pressure difference, Pa. The parameters $A(k_0)$ and $B(k_0)$ can be calculated by:

$$A(k_0) = ak_0^b \tag{2}$$

$$B(k_0) = ck_0^d + e \tag{3}$$

where a, b, c, d and e are the coefficients.

2.3 TPG experiments and analysis

Four cores were selected from tight gas reservoirs in Ordos Basin, China. The porosity and permeability of the cores were measured by a helium pycnometer (Mergia et al., 2010; Pan et al., 2021) and the pressure decay method (Wu et al., 2020), respectively, The core properties are shown in Table 1. As can be seen in Table 1, the permeability of sample 1# and sample 2# were outside the range of tight gas reservoirs. These two cores were selected to experimentally demonstrate the general applicability of the subsequently derived TPG equation.

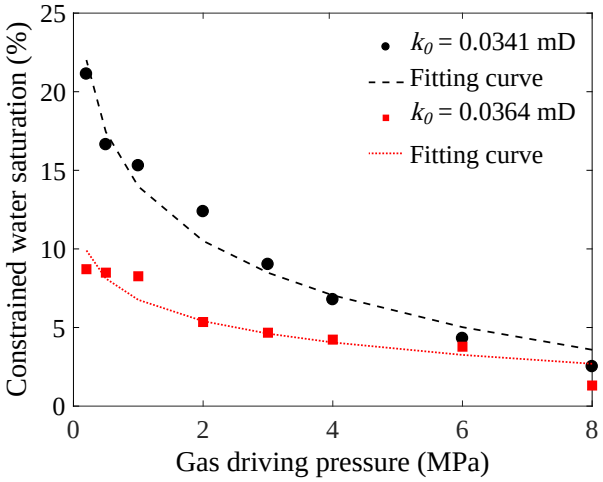

Fig. 2. Constrained water saturation as a function of gas driving pressure for core with various permeabilities.

Table 1. The core properties.

Sample	Diameter (cm)	Length (cm)	Porosity (%)	Permeability (mD)
1#	2.550	3.606	15.16	9.02
2#	2.550	6.480	14.20	1.51
3#	2.538	5.056	13.11	0.687
4#	2.540	5.600	10.62	0.052

TPG was measured by the method of differential pressure-flow (Dong et al., 2019; Song et al., 2019; Abdulkadir et al., 2020). The TPG curves of cores with different permeabilities and at different water saturations are shown in Fig. 3. TPG increased with the increase of total water saturation and with the decrease of core permeability.

Based on previous studies on TPG, mathematical models analyzing the characteristics and laws of non-linear flow under the TPG effect have been abundant (Guo et al., 2012; Wang and Sheng, 2017). For the Sulige gas field, Yang et al. (2015) combined the bubble method and differential pressure-flow method and put forward the TPG equation affected by water saturation and permeability. On the basis of the equation, Tian et al. (2018) obtained the TPG equation that considers permeability, connate water and movable water from experimental data. With the course of time, the constrained water is released from the small pore space, the space for gas flow increases, and the resistance to flow decreases. To accurately describe the effect of constrained water saturation on TPG, by taking the above equation and combining it with Eq. (1), the TPG equation considering S_{wc} and permeability can be obtained:

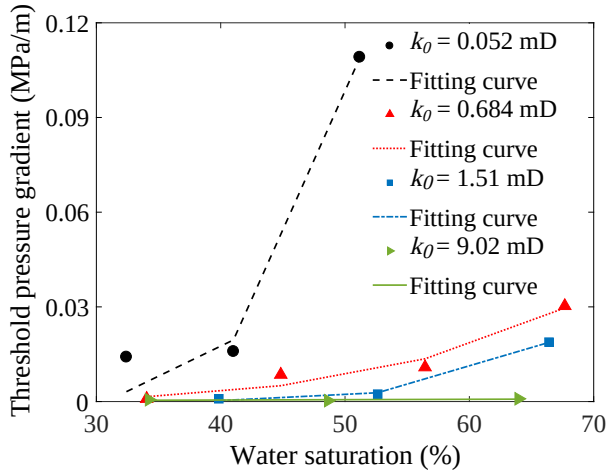

Fig. 3. TPG curve under different water saturations.

$$G = \alpha k_0^{-\beta} (S_{wi} - S_{wc})^{\gamma} \tag{4}$$

where G denotes the TPG, Pa/m; α, β, γ are coefficients; S_{wi} denotes initial water saturation, %.

3. Mathematical model and sensitivity analysis of production

3.1 Model derivation

3.1.1 Basic assumptions

The reservoir is horizontal, homogeneous, has equal thickness, and is isotropic. The fluid seepage process is isothermal and does not consider the effects of gravity and capillary forces. The porosity of the reservoir is constant. The gas reservoir contains water, the flow of water phase is discontinuous, and no physical and chemical reactions occur between gas and water. There is a slip effect on gas-phase seepage and a stress sensitivity regarding the absolute permeability of the reservoir. According to previous studies, TPG is a function of water saturation and permeability.

3.1.2 Model formulation

The continuity equation is:

$$-\nabla(\rho_g v) = 0 \tag{5}$$

where ρ_g denotes gas density, kg/m^3; v denotes gas flow rate, m/s.

Under isothermal conditions, the density of gas is obtained:

$$\rho_g = \frac{T_s Z_s \rho_{gs}}{p_s} \frac{p}{TZ} \tag{6}$$

where p denotes reservoir pressure, Pa; T_s denotes temperature under standard state, K; Z_s denotes gas compression operator under standard state; ρ_{gs} denotes gas density under standard state, kg/m^3; p_s denotes pressure under standard state, Pa; T denotes formation temperature, K; Z denotes gas compression operator.

The motion equation considering the TPG is:

$$v = -\frac{k_g}{\mu}\left(\frac{\partial p}{\partial r} - G\right) \tag{7}$$

where k_g denotes gas permeability, mD; μ denotes gas viscosity, Pa/s; r denotes distance from shaft, m.

The permeability varies with effective stress, which is significant in tight gas reservoirs (Zhong et al., 2020). There is a slippage effect in the gas flow (Li et al., 2018). Considering this effect, as well as stress sensitivity and diffusion under the influence of pressure, the permeability is corrected as:

$$k_g = k_0 e^{\lambda(p_e - \bar{p})}\left(1 + \frac{3\pi f}{16 k_0}\frac{\mu D_p}{\bar{p}}\right)\left(1 + \frac{g}{\bar{p}}\right) \tag{8}$$

where p_e denotes initial reservoir pressure, Pa; $\bar{p}$ denotes average reservoir pressure, Pa; D_p denotes diffusion coefficient with pressure, m^2/s; λ, f, g are coefficients.

By substituting Eq. (1) into Eq. (4), the following equation is obtained:

$$G = \alpha k_0^{-\beta}\left[S_{wi} - A(k_0)\ln(\Delta p) - B(k_0)\right]^{\gamma} \tag{9}$$

By substituting Eq. (5) into Eq. (7), the following seepage differential equation is obtained:

$$-\nabla\left[\rho_g \frac{k_g}{\mu}\left(\frac{\partial p}{\partial r} - G\right)\right] = 0 \tag{10}$$

Combining (10) with (6) yields:

$$\frac{T_s Z_s \rho_{gs} k_g}{P_s T}\nabla\left[\rho_g \frac{p}{\mu Z}\left(\frac{\partial p}{\partial r} - G\right)\right] = 0 \tag{11}$$

Then, the pseudo pressure function is introduced:

$$m = 2\int_{\varphi_w}^{\varphi} \frac{\varphi + G(r - r_w)}{\mu Z} d\varphi \tag{12}$$

where r_w denotes the radius of the wellbore, m; m is pseudo pressure, Pa; $\varphi = p - G(r - r_w)$.

The equation for the pseudo pressure distribution in polar coordinates of the plane radial flow is:

$$\frac{\mathrm{d}^2 m}{\mathrm{d}r^2} + \frac{1}{r}\frac{\mathrm{d}m}{\mathrm{d}r} = 0 \tag{13}$$

The inner boundary condition:

$$r = r_w, p = p_{wf} \tag{14}$$

The outer boundary condition:

$$r = r_e, p = p_e \tag{15}$$

where p_{wf} denotes the pressure of the wellbore, Pa; r_e denotes the radius of the boundary, m.

By substituting Eq. (14) and Eq. (15) into Eq. (13), the pressure distribution can be expressed as:

$$p = \sqrt{p_{wf}^2 + G^2(r_e - r_w)^2 + \frac{p_e^2 - p_{wf}^2 - G^2(r - r_w)^2}{\ln r_e - \ln r_w}\ln\frac{r}{r_w}} \tag{16}$$

The production rate (q) in the matrix is as follows:

$$q = \frac{\pi k_g h T_s Z_s \rho_{gs}}{p_s T}\frac{p_e^2 - p_{wf}^2 - G^2(r_e - r_w)^2}{\ln r_e - \ln r_w} \tag{17}$$

where h denotes reservoir thickness, m.

3.2 Dynamic pressure propagation in a tight gas reservoir

3.2.1 Average reservoir pressure equation

The average reservoir pressure is calculated by the area weighted average method:

$$\bar{p} = \frac{1}{A}\int 2\pi p r \mathrm{d}r \tag{18}$$

where A denotes effective utilization area, m^2.

Using Eq. (18), the average reservoir pressure can be obtained:

$$\bar{p} = \sqrt{p_{wf}^2 + \frac{G^2}{6}\frac{3r^3 - 5r^2 r_w + r r_w^2 + r_w^3}{r + r_w} + \frac{p_e^2 - p_{wf}^2 - G^2(r_e - r_w)^2}{2(\ln r - \ln r_w)}\left[\frac{r^2(\ln r^2 - \ln r_w^2)}{r^2 - r_w^2} - 1\right]} \tag{19}$$

3.2.2 Dynamic pressure propagation law

Based on the material balance method, the cumulative production rate is equal to the pore volume change within the effective range of the tight reservoir (Zhu et al., 2011, 2016):

$$\sum_{t=1}^{n} Q_t = \int_{r_w}^{r} 2\pi r h\left[(\rho_g \phi)_i - (\rho_g \phi)\right] dr \tag{20}$$

where Q_t denotes production rate with time, m^3/s; ϕ denotes porosity; subscript i denotes initial condition.

Solving Eq. (20) yields:

$$\sum_{t=1}^{n} Q_t = \pi h \phi C_t (r^2 - r_w^2)(p_e - \bar{p}) \tag{21}$$

where C_t denotes reservoir total compressibility, Pa^{-1}.

Based on the steady-state sequential substitution method, the non-steady-state flow process is a sequential substitution of steady states, and the difference in the steady state at each time step is the supply radius. The specific steps are as follows: Based on the material balance method, Eq. (17) and Eq. (21) can be used to calculate the dynamic supply radius r and the production rate q and Q_t at time t; Then, the average reservoir pressure $\bar{p}$ can be calculated according to Eq. (19).

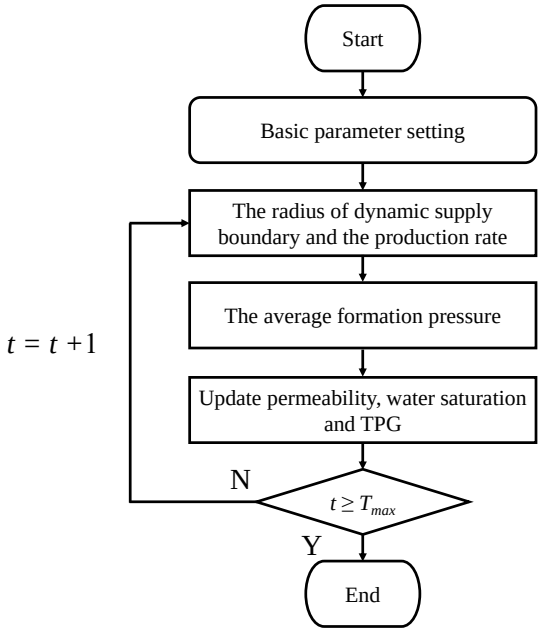

Fig. 4. Workflow for water-bearing tight gas reservoir considering the effect of the TPG seepage model.

Table 2. Basic parameters in tight gas reservoirs.

Parameter	Value
Initial reservoir pressure (Pa)	25×10^6
Bottom hole flowing pressure (Pa)	5×10^6
Porosity (%)	20
Premeability (mD)	0.25, 0.2, 0.15, 0.1
Initial water saturation (%)	80, 70, 60, 50
Gas viscosity (Pa·s)	2.7×10^{-5}
Rock compressibility (1/Pa)	7×10^{-10}
Effective thickness (m)	15
Radius of the boundary (m)	300
Radius of the wellbore (m)	0.1

At the same time, S_{wc} is modified by Eq. (1), TPG is modified by Eq. (4), and k_g is modified by Eq. (8); Subsequently, the modified permeability k_g and TPG are treated as known parameters for the next time step, and the supply radius of pressure propagation is calculated at the next time step and iterated. The detailed workflow of this study is presented in Fig. 4.

3.3 Sensitivity analysis of parameters

The basic parameters are shown in Table 2. These values are all substituted into mathematical model to predict the production rate and dynamic supply boundary.

3.3.1 Effect of TPG

In order to investigate the effect of TPG on gas production performance, the gas production rate and cumulative gas production rate versus production time were plotted in Figs. 5(a) and 5(b), respectively. If the TPG is considered as constant, the value is 0.041 MPa/m (calculated by Eq. (6)), and the gas production rate decreases from 5.85×10^4 to 4.35×10^4 m^3/d with the increase in production time from 0 to 2,000. In contrast, if the TPG is not constant (calculated by Eq. (6)), the gas production rate decreases from 5.85×10^4 to 4.89×10^4 m^3/d with the increase in production time from 0 to 2,000. It is clearly seen that more than 11% and 6.44% difference in the gas production rate and cumulative gas production rate exist for a constant and a non-constant TPG, respectively. The TPG is a parameter that varies with permeability and water saturation. When the production time increases, the permeability and water saturation decrease, thus TPG is a variable parameter.

During the seepage of tight gas reservoir, affected by the TPG, the pressure will not be transmitted to the reservoir boundary instantaneously, but will gradually expand outward with the passage of time, hence the pressure propagation boundary is called dynamic supply boundary (Zhu et al., 2016). As shown in Fig. 6, when the TPG is constant, the dynamic supply boundary propagates to 112 m after 2,000 days, and when the TPG changes with the production time, the dynamic supply boundary propagates to 122 m after 2,000

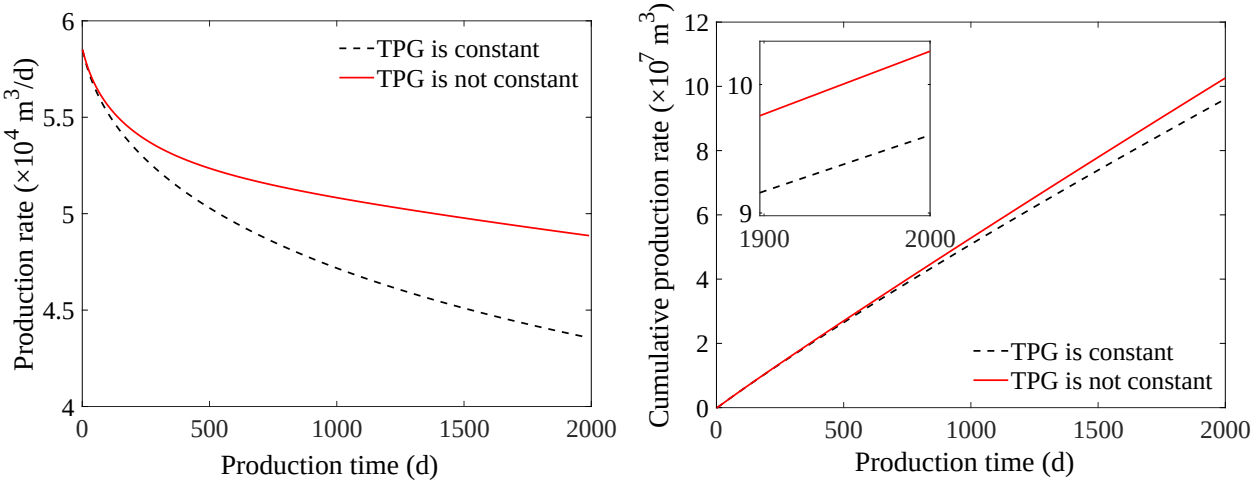

Fig. 5. (a) Gas production rate and (b) cumulative gas production as a function of production time in tight reservoirs.

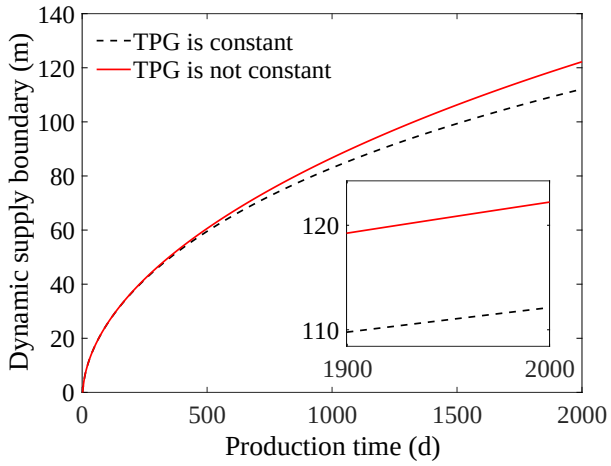

Fig. 6. Dynamic supply boundaries in tight reservoirs at different permeabilities.

days. The calculated result shows that, if the TPG is considered as constant, the utilization area is small.

3.3.2 Effect of permeability

The influence of permeability (0.1, 0.15, 0.2, and 0.25 mD) on the gas production rate during the natural energy development process was simulated over a period of 2,000 days. As can be seen from Fig. 7, as the permeability decreases uniformly from 0.25 to 0.1 mD, the production rate curve progressively decreases (Fig. 7(a)), with this trend, the decline rates of cumulative gas production rate for 2,000 days are 2.44%, 3.7%, and 6.75%, respectively (Fig. 7(b)). When the permeability is less than 0.15 mD, the gas production decreases significantly. According to the previous analysis of TPG, decreased permeability leads to reduced porosity, lowered proportion of large pores in the core and increased proportion of small pores (Chen et al., 2020), resulting in an increase in TPG (Fig. 7(c)). This will increase the resistance to gas flow, reduce the gas transport performance, shorten the dynamic supply boundary propagation distance and reduce the supply area (Fig. 7(d)), such that the production will dwindle with the decrease of permeability.

3.3.3 Effect of initial water saturation

The influence of initial water saturation (80%, 70%, 60%, and 50%) on the gas rate during the natural energy development process was simulated over a period of 2,000 days. As can be seen from Fig. 8, when the initial water saturation decreases uniformly from 80% to 50%, the gas production rate curve decreases, which effect mainly occurs before 1,500 days (Fig. 8(a)) and the cumulative gas production rate decrease is 1% over 2,000 days in all these cases (Fig. 8(b)). The effect of initial water saturation on gas production rate mainly takes place in the intermediate stage during production. High initial water saturation inhibits gas flow in the pore space (Fu et al., 2022), and the water phase in porous media forms a continuous water film on the pore walls, reducing the effective gas flow space. This corresponds to a reduction in gas permeability and an increase in fluid flow resistance, subjecting the greater TPG during flow (Fig. 8(c)), and making the TPG vary considerably between the pre-production and mid-production periods, similar to the variation in production rate. At the same time, although initial water saturation has an obvious effect on gas production, it has little effect on the dynamic supply boundary (Fig. 8(d)).

4. Conclusions

Based on the results presented above, the following conclusions are drawn:

1) The further delineation of the water state in a tight gas reservoir is as follows: movable water, irreducible water and constrained water. The relationship of constrained water saturation and permeability with critical driving pressure difference was proposed. Then, a prediction equation for the variable TPG considering the constrained water saturation was developed.

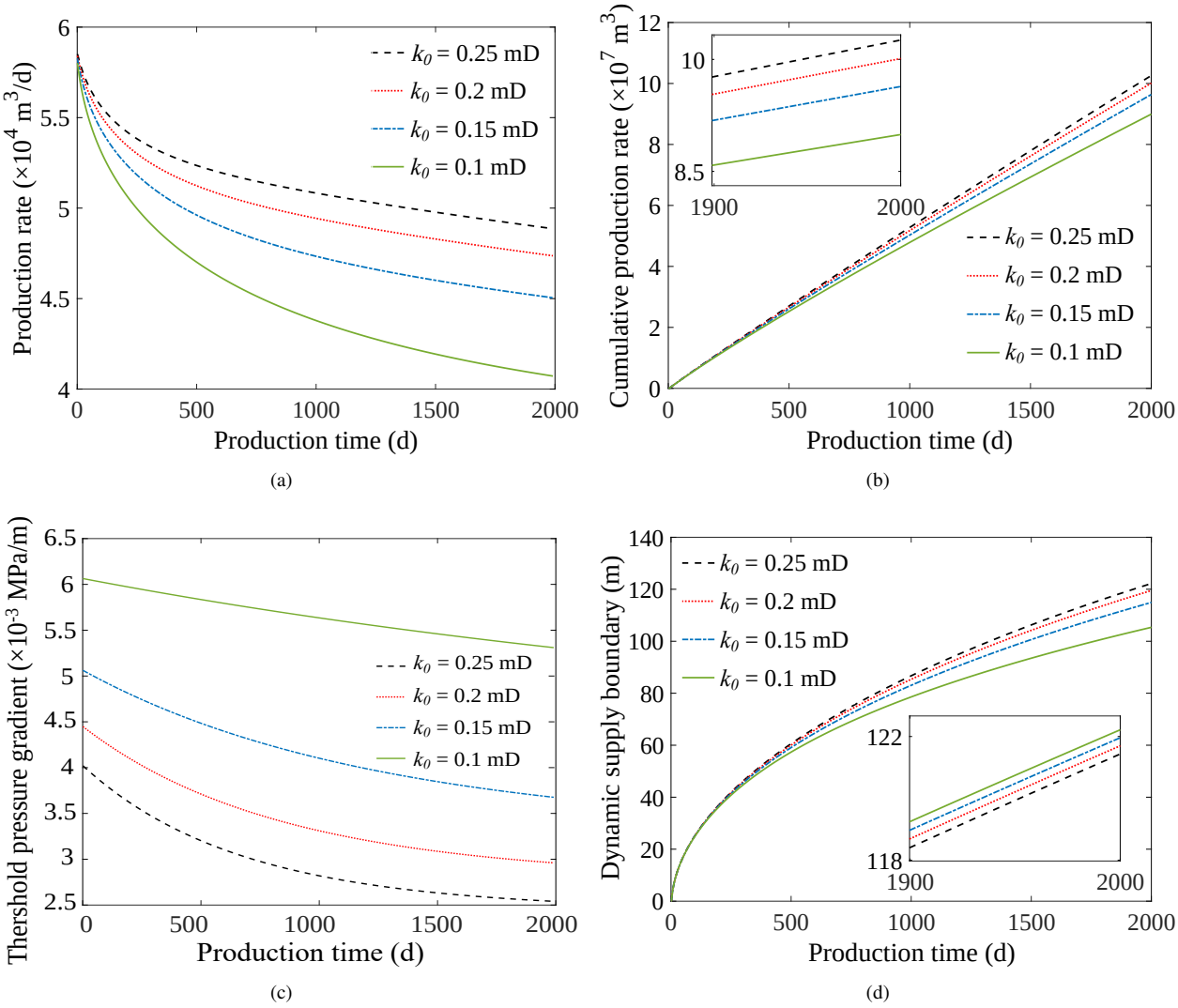

Fig. 7. Production under different permeabilities. (a) Effect of permeability on production rate; (b) Effect of permeability on cumulate production; (c) Effect of permeability on TPG; and (d) Effect of permeability on dynamic supply boundary.

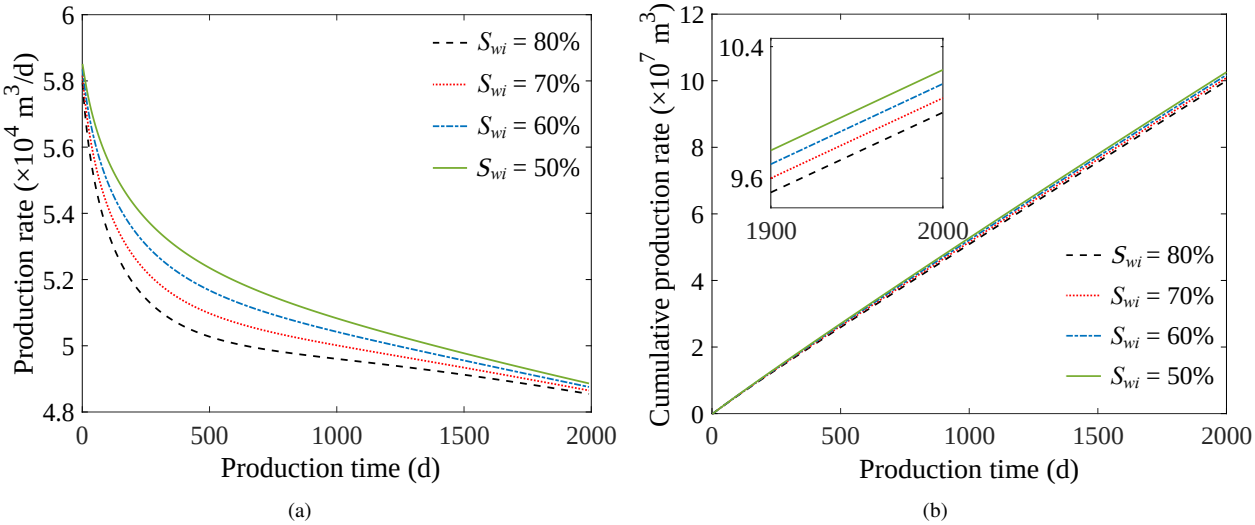

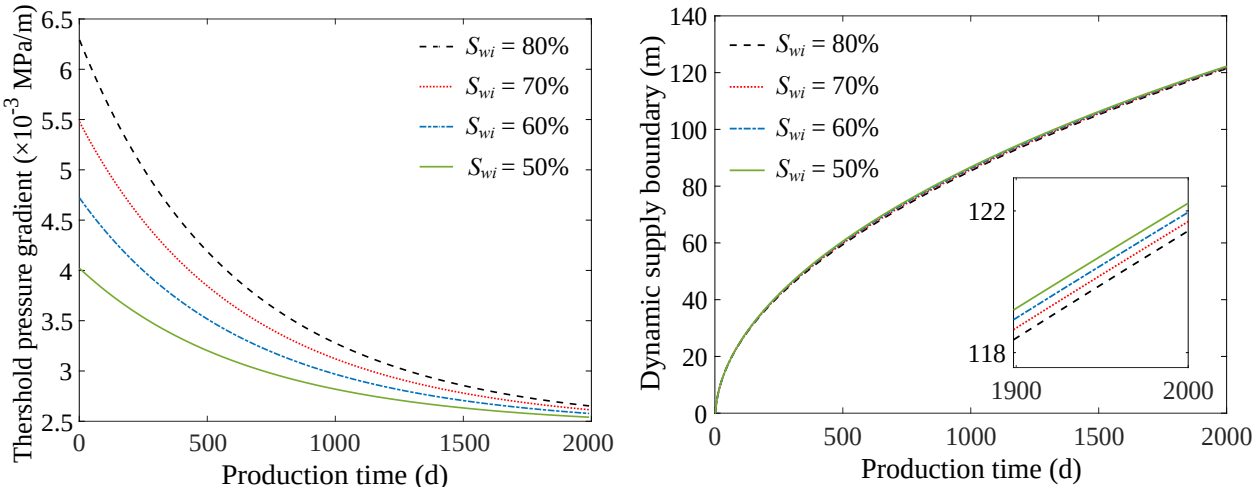

Fig. 8. Production with different initial water saturation levels. (a) Effect of initial water saturation on production rate; (b) Effect of initial water saturation on cumulate production; (c) Effect of initial water saturation on TPG; and (d) Effect of initial water saturation on dynamic supply boundary.

2) A production prediction model considering variable TPG was established. With the development time, the TPG decreases, the gas production rate is 11.11% larger, and the cumulative gas production rate is 8.33% greater than when the TPG is constant. In the latter case, the calculation results demonstrate a weaker gas production capacity of the reservoir than the actual scenario.
3) The dynamic supply boundary model considering the variable TPG was obtained. It was found that the permeability has a great influence on the dynamic supply boundary, on which the initial water saturation has almost no influence. Therefore, the reservoir should be fractured at the early stage of production development to increase the permeability and reduce the initial water saturation at the same time.

Acknowledgement

The authors acknowledge the financial support from the Natural Sciences for Youth Foundation of China (No. 42102163) and the Fundamental Research Funds of the Central Universities (No. FRF-TP-20-006A1). The authors would also like to thank the reviewers and editors whose critical comments were very helpful for the preparation of this article.

Conflict of interest

The authors declare no competing interest.

References

Abdulkadir, M., Jatto, D. G., Abdulkareem, L. A., et al. Pressure drop, void fraction and flow pattern of vertical air-silicone oil flows using differential pressure transducer and advanced instrumentation. Chemical Engineering Research and Design, 2020, 159: 262-277.

Afagwu, C., Alafnan, S., Mahmoud, M. A., et al. Permeability model for shale and ultra-tight gas formations: Critical insights into the impact of dynamic adsorption. Energy Reports, 2021, 7: 3302-3316.

Akilu, S., Padmanabhan, E., Sun, Z. A review of transport mechanisms and models for unconventional tight shale gas reservoir systems. International Journal of Heat and Mass Transfer, 2021, 175: 121125.

Cai, J. A fractal approach to low velocity non-Darcy flow in a low permeability porous medium. Chinese Physics B, 2014, 23(4): 044701.

Castro, T. M. D., Lupinacci, W. M. Comparison between conventional and NMR approaches for formation evaluation of presalt interval in the Buzios Field, Santos Basin, Brazil. Journal of Petroleum Science and Engineering, 2022, 208: 109679.

Chai, X., Tian, L., Dong, P., et al. Study on recovery factor and interlayer interference mechanism of multilayer co-production in tight gas reservoir with high heterogeneity and multi-pressure systems. Journal of Petroleum Science and Engineering, 2022, 210: 109699.

Chen, H., Li, H., Li, Z., et al. Effects of matrix permeability and fracture on production characteristics and residual oil distribution during flue gas flooding in low permeability/tight reservoirs. Journal of Petroleum Science and Engineering, 2020, 195: 107813.

Dong, M., Yue, X., Shi, X., et al. Effect of dynamic pseudo threshold pressure gradient on well production performance in low-permeability and tight oil reservoirs. Journal of Petroleum Science and Engineering, 2019, 173: 69-76.

Durucan, S., Ahsan, M., Shi, J., et al. Two phase relative permeabilities for gas and water in selected European

coals. Fuel, 2014, 134: 226-236.

El Sharawy, M. S., Gaafar, G. R. Impacts of petrophysical properties of sandstone reservoirs on their irreducible water saturation: Implication and prediction. Journal of African Earth Sciences, 2019, 156: 118-132.

Fu, J., Su, Y., Li, L., et al. Productivity model with mechanisms of multiple seepage in tight gas reservoir. Journal of Petroleum Science and Engineering, 2022, 209: 109825.

Gao, Y., Chen, S., Huang, F., et al. Micro-occurrence of formation water in tight sandstone gas reservoirs of low hydrocarbon generating intensity: Case study of northern Tianhuan Depression in the Ordos Basin, NW China. Journal of Natural Gas Geoscience, 2021, 6(4): 215-229.

Guo, J., Zhang, S., Zhang, L., et al. Well testing analysis for horizontal well with consideration of threshold pressure gradient in tight gas reservoirs. Journal of Hydrodynamics, 2012, 24(4): 561-568.

Han, G., Liu, Y., Nawnit, K., et al. Discussion on seepage governing equations for low permeability reservoirs with a threshold pressure gradient. Advances in Geo-Energy Research, 2018, 2(3): 245-259.

Hossain, Z., Grattoni, C. A., Solymar, M., et al. Petrophysical properties of greensand as predicted from NMR measurements. Petroleum Geoscience, 2011, 17(2): 111-125.

Imani, G., Zhang, L., Blunt, M. J., et al. Quantitative determination of the threshold pressure for a discontinuous phase to pass through a constriction using microscale simulation. International Journal of Multiphase Flow, 2022, 153: 104107.

Kong, D., Lian, P., Zhu, W., et al. Pore-scale investigation of immiscible gas-assisted gravity drainage. Physics of Fluids, 2020, 32(12): 122004.

Li, J., Chen, Z., Wu, K., et al. Effect of water saturation on gas slippage in tight rocks. Fuel, 2018, 225(1): 519-532.

Li, Y., Hu, Z., Cai, C., et al. Evaluation method of water saturation in shale: A comprehensive review. Marine and Petroleum Geology, 2021, 128: 105017.

Li, X., Liang, J., Xu, W., et al. The new method on gas-water two phase steady-state productivity of fractured horizontal well in tight gas reservoir. Advances in Geo-Energy Research, 2017, 1(2): 105-111.

Liu, W., Wu, Z., Li, J., et al. The seepage characteristics of methane hydrate-bearing clayey sediments under various pressure gradients. Energy, 2020, 191: 116507.

Mahdi, D. S., Al-Khdheeawi, E. A., Yuan, Y., et al. Hydrogen underground storage efficiency in a heterogeneous sandstone reservoir. Advances in Geo-Energy Research, 2021, 5(4): 437-443.

McGlade, C., Speirs, J., Sorrell, S. Unconventional gas-A review of regional and global resource estimates. Energy, 2013, 55: 571-584.

Mejia, L., Mejia, M., Xie, C., et al. Viscous fingering of irreducible water during favorable viscosity two-phase displacements. Advances in Water Resources, 2021, 153: 103943.

Meng, D., Jia, A., Ji, G., et al. Water and gas distribution and its controlling factors of large scale tight sand gas fields: A case study of western Sulige gas field, Ordos Basin, NW China. Petroleum Exploration and Developmen, 2016, 43(4): 663-671.

Mergia, K., Stefanopoulos, K. L., Ordás, N., et al. A comparative study of the porosity of doped graphites by small angle neutron scattering, nitrogen adsorption and helium pycnometry. Microporous and Mesoporous Materials 2010, 134(1-3): 141-149.

Miller, R. J., Low, P. F. Threshold gradient for water flow in clay systems. Soil Science Society of America Journal, 1963, 27(6): 605-609.

Muskat, M., Meres, M. W. The flow of heterogeneous fluids through porous media. Physics, 1936, 7(9): 346-363.

Ning, B., Xiang, Z., Liu, X., et al. Production prediction method of horizontal wells in tight gas reservoirs considering threshold pressure gradient and stress sensitivity. Journal of Petroleum Science and Engineering, 2020, 187: 106750.

Pan, B., Clarkson, C. R., Debuhr, C., et al. Low-permeability reservoir sample wettability characterization at multiple scales: Pore-, micro- and macro-contact angles. Journal of Natural Gas Science and Engineering, 2021, 95: 104229.

Parda, A., Civan, F. Modification of Darcy's law for the threshold pressure gradient. Journal of Petroleum Science and Engineering, 1999, 22(4): 237-240.

Pertsin, A., Grunze, M. Water-graphite interaction and behavior of water near the graphite surfaced. Journal of Physical Chemistry B, 2004, 108(4): 1357-1364.

Shar, A. M., Mahesar, A. A., Chandio, A. D., et al. Impact of confining stress on permeability of tight gas sands: An experimental study. Journal of Petroleum Exploration and Production Technology, 2016, 7(3): 717-726.

Shilov, E., Dorhjie, D. B., Mukhina, E., et al. Experimental and numerical studies of rich gas Huff-n-Puff injection in tight formation. Journal of Petroleum Science and Engineering, 2022, 208: 109420.

Song, F., Bo, L., Zhang, S., et al. Nonlinear flow in low permeability reservoirs: Modelling and experimental verification. Advances in Geo-Energy Research, 2019, 3(1): 76-81.

Szabó, N. P., Remeczki, F., Jobbik, A., et al. Interval inversion based well log analysis assisted by petrophysical laboratory measurements for evaluating tight gas formations in Derecske through, Pannonian basin, east Hungary. Journal of Petroleum Science and Engineering, 2022, 208: 109607.

Taktak, F., Rigane, A., Boufares, T., et al. Modelling approaches for the estimation of irreducible water saturation and heterogeneities of the commercial Ashtart reservoir from the gulf of Gabès, Tunisia. Journal of Petroleum Science and Engineering, 2011, 78(2): 376-383.

Tian, W., Li, A., Ren, X., et al. The threshold pressure gradient effect in the tight sandstone gas reservoirs with high water saturation. Fuel, 2018, 226: 221-229.

Verdugo, M., Doster, F. Impact of capillary pressure and flowback design on the clean up and productivity of hydraulically fractured tight gas wells. Journal of Petroleum

Science and Engineering, 2022, 208: 109465.

Wang, X., Sheng, J. J. Discussion of liquid threshold pressure gradient. Petroleum, 2017, 3(2): 232-236.

Wu, T., Zhang, D., Li, X. A radial differential pressure decay method with micro-plug samples for determining the apparent permeability of shale matrix. Journal of Natural Gas Science and Engineering, 2020, 74: 103126.

Xin, Y., Wang, G., Liu, B., et al. Pore structure evaluation in ultra-deep tight sandstones using NMR measurements and fractal analysis. Journal of Petroleum Science and Engineering, 2022, 211: 110180.

Yang, Z., Li, X., Liu, S., et al. Threshold pressure effect of low permeability tight gas reservoirs in Sulige gas field. Acta Petrolei Sinica, 2015, 36(3): 347-354.

Zeng, B., Cheng, L., Hao, F. Experiment and mechanism analysis on threshold pressure gradient with different fluids. Paper SPE 140678 Presented at Nigeria Annual International Conference and Exhibition, Tinapa-Calabar, Nigeria, 31 July-7 August, 2010.

Zhang, J., Li, X., Shen, W., et al. Study of the effect of movable water saturation on gas production in tight sandstone gas reservoirs. Energies, 2020, 13(18): 4645.

Zhao, W., Zhang, T., Jia, C., et al. Numerical simulation on natural gas migration and accumulation in sweet spots of tight reservoir. Journal of Natural Gas Science and Engineering, 2020, 81: 103454.

Zhong, X., Zhu, Y., Liu, L., et al. The characteristics and influencing factors of permeability stress sensitivity of tight sandstone reservoirs. Journal of Petroleum Science and Engineering, 2020, 191: 107221.

Zhu, W., Liu, Y., Li, Z., et al. Study on pressure propagation in tight oil reservoirs with stimulated reservoir volume development. ACS Omega, 2021, 6(4): 2589-2600.

Zhu, W., Qi, Q., Ma, Q., et al. Unstable seepage modeling and pressure propagation of shale gas reservoirs. Petroleum Exploration and Development, 2016, 43(2): 285-292.

Zhu, W., Song, H., Huang, X., et al. Pressure characteristics and effective deployment in a water-bearing tight gas reservoir with low-velocity non-darcy flow. Energy & Fuels, 2011, 25(3): 1111-1117.

Zou, C., Zhu, R., Liu, K., et al. Tight gas sandstone reservoirs in China: Characteristics and recognition criteria. Journal of Petroleum Science and Engineering, 2012, 88-89: 82-91.